Fast automated non-linear contour propagation for adaptive head and neck radiotherapy.

Florian Weiler[1], Christoph Brachmann[1], Nadine Traulsen[2], Reinoud Nijhuis[3], Grzegorz Chlebus[1], Mark Schenk[2], Dörte Corr[1], Stefan Wirtz[1], Ute Ganswindt[3], Christian Thieke[3], Claus Belka[3], and Horst K. Hahn[1]

[1] Fraunhofer MEVIS, Universitätsallee 29, 28359 Bremen, Germany.
[2] Fraunhofer MEVIS, Maria-Goeppert-Straße 3, 23562 Lübeck, Germany.
[3] Ludwig-Maximilians-University, Department of Radiation Oncology, Munich, Germany.
florian.weiler@mevis.fraunhofer.de

Abstract. A crucial and time-consuming task in adaptive radiotherapy is the propagation of contours from an initial planning CT image to a control image taken during the course of treatment. Precise adaptation of contours for organs at risk, as well as target volumes is necessary in order to calculate an adapted treatment plan. Although several commercially available solutions exist that aim at solving this task, manual editing and correction of such automated mappings is still an inevitable requirement making the overall process tedious and time-consuming in clinical routine. We present a processing pipeline aiming at fast and fully automated propagation of contours between different datasets of an ongoing therapy. The method is based on a non-linear image registration combined with GPU accelerated contour generation. We evaluate our method by calculating Dice similarity coefficients and 3D Hausdorff distances between our results, and manually generated contours which serve as a ground truth. Additionally, we compare our results against contours mapped using a state-of-the-art commercially established contouring software.

Keywords: Adaptive radiotherapy, contour propagation, non-linear registration

1 Introduction

Adaptive radiotherapy attempts to improve the outcome of radio-therapeutic tumor treatment by adapting an original treatment-plan during the course of therapy to physiological changes occurring in the patients body. To facilitate this, CT-imaging is performed at certain stages during therapy, building the foundation for adaptation of the treatment plan. In order to calculate an adapted plan, contours of both target structures as well as organs at risk need to be transferred to the control CT image, taking into account the current anatomical situation.

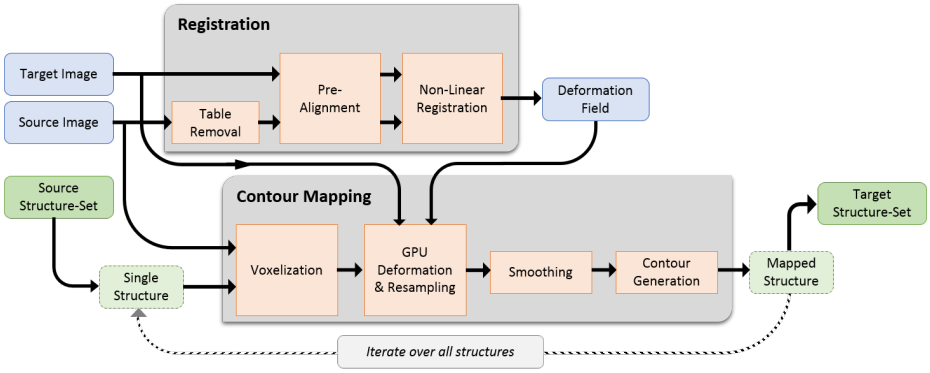

Fig. 1. Overview of the complete processing pipeline.

This goal can theoretically be achieved in two ways. First, the control CT could be completely re-contoured, resulting in a new set of contours, independent of the initial structures. Alternatively, the original structures can be transferred to the target image by means of non-linear image registration with subsequent transformation of all structures. The latter approach offers two significant advantages: First, the time requirement can be reduced given the fact that a well fitting set of contours builds the basis for typically required corrections. Second, the correspondence between structures from the planning image to the control image remains intact, facilitating precise calculations of volumetric changes of individual structures over time.

Both approaches are supported by current commercially available software systems such as ABAS [1]. Complete re-contouring is supported by means of multi-atlas based pre-segmentation of organs at risk, followed by inevitable manual adaptations of the resulting contours. Alternatively, the original contours can be used for a single-atlas based segmentation.

In this paper, we present a novel approach for fully automated transfer of contours from different CT images relying on a non-linear image registration with automatic patient table removal, followed by re-generation of contours of the original structures on the target image. We evaluate our method by comparing the results of the mapping process to those obtained using ABAS.

2 Methods

Our method is based on a processing-pipeline consisting of two main stages: First, the non-linear image registration and second the image based contour mapping. The registration stage consists of a pre-processing step aiming at automatic table removal, followed by a coarse linear volume alignment with subsequent non-linear image registration as presented in [4]. The mapping stage consists of structure voxelization, GPU accelerated deformation and resampling, and finally contour

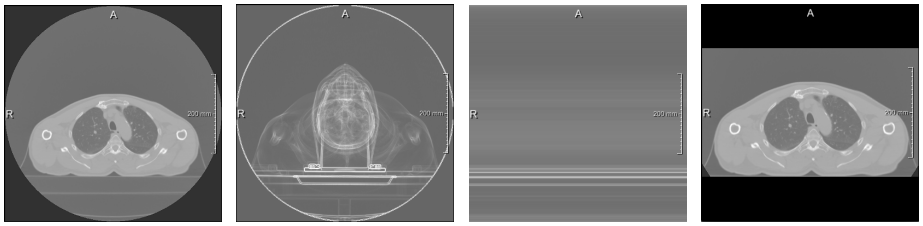

(a) (b) (c) (d)

Fig. 2. A representative slice of the input image volume is displayed in (a). The projection along the z-axis results in (b), and a further projection along the x-axis in (c). (d) displays the resulting cropped output image after automatic table removal.

generation using the marching squares approach. Figure 1 gives a schematic overview of the complete pipeline.

2.1 Automatic table removal

To eliminate the influence of the CT scanning table on the results of the image registration, we have implemented a simple technique for table removal. As an exact registration of the patient table would have no impact on the addressed problem, a VOI including the patient volume only is automatically calculated. This eliminates the influence of structures outside the patient on the distance measure and also reduces computation costs effectively speeding up the registration process as the considered image domain Ω is reduced to the VOI only.

The proposed method is derived from [9], but has been adapted to images used in radiotherapy. We exploit the circumstance that the patient table is typically aligned in parallel to the direction of image acquisition. This allows to easily identify the table by performing an orthogonal projection of locally maximal image intensities along the z-axis of the input image. This sums up all table voxels, forming a very dominant line in the projected image. A second projection along the x-axis generates a one-dimensional image profile, where the maximum image intensity depicts the surface of the table. Figure 2 gives a short overview of the performed steps.

2.2 Non-linear image registration

One of our general expectation regarding the non-linear, intra-patient image registration here is, that the deformations will be considered as smooth. The future-oriented trend of standardized patient positioning in advanced head and neck radiotherapy supports this assumption. Therefore, we chose the Normalized Gradient Fields (NGF) [3] as distance measure, focusing on edges in the CT images to be registered, and a curvature regularizer, aiming for smooth deformations.

Consider $\mathcal{R} : \mathbb{R}^3 \to \mathbb{R}$ as the fixed reference image and $\mathcal{T} : \mathbb{R}^3 \to \mathbb{R}$ as the moving template image with compact support in domain $\Omega \subseteq \mathbb{R}^3$. Image registration aims to find a transformation $y : \Omega \to \mathbb{R}^3$ such that $\mathcal{T}(y)$ is similar to $\mathcal{R}$. In our specific application of contour propagation we aim to be able to propagate contours as images with the transformation y.

The variational approach used for the non-linear image registration step here, models the image registration process by the objective function $\mathcal{J}$

$$\mathcal{J} = \mathcal{D}(\mathcal{R}, \mathcal{T}(y)) + \alpha \cdot \mathcal{S}(y), \tag{1}$$

where $\mathcal{D}$ is the distance measure, $\mathcal{S}$ is the regularizer, and α is the regularization parameter, a weighting factor affecting data fit and regularity.
We used the Normalized Gradient Fields (NGF) [3] as distance measure. For $x \in \Omega$ it is given by

$$\mathcal{D}(\mathcal{R}, \mathcal{T}(y)) := \int_{\Omega} 1 - \left(\frac{\langle \nabla \mathcal{T}(y(x)), \nabla \mathcal{R}(x) \rangle_\eta}{\| \nabla \mathcal{T}(y(x)) \|_\eta \| \nabla \mathcal{R}(x) \|_\eta} \right)^2 \mathrm{d}x \tag{2}$$

with

$$\langle f, g \rangle_\eta := \sum_{j=1}^{3} f_j g_j + \eta^2 \quad \text{and} \quad \|f\|_\eta := \sqrt{\langle f, f \rangle_\eta} \tag{3}$$

to describe image similarity. The NGF distance measure considers the angle between image gradient vectors in the reference and the template image at each point. The edge parameter η is used to define a threshold, that specifies which gradients are counted among the noise level.

For regularization purpose we used the curvature regularizer as proposed in [2], which is based on second order derivatives, penalizing the Laplacian of the displacement components. The curvature regularizer $\mathcal{S}$ is given by

$$\mathcal{S}(y) := \frac{1}{2} \sum_{l=1}^{3} \int_{\Omega} \|\Delta u\|^2 \mathrm{d}x \tag{4}$$

with the decomposition $y(x) = x + u(x)$, where u is the displacement. One beneficial characteristic of the curvature regularizer is, that it results in very smooth deformations, meeting our expectations.

A discretize-then-optimize scheme [5] is performed to optimize $\mathcal{J}$ using a quasi-Newton L-BFGS optimizer [7]. To avoid local minima, the iteration scheme is embedded into a multi-level approach [5]. Therefore, the optimization problem is solved consecutively on coarse to fine image resolution levels. In this implementation, the objective function is evaluated on 5 levels. The proposed results were obtained with an edge parameter of $\eta = 0.1$ and a regularization parameter of $\alpha = 1$.

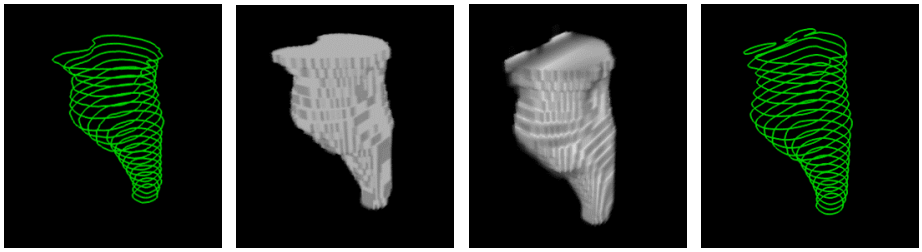

(a) (b) (c) (d)

Fig. 3. Illustration of the mapping process: Axial source contours (a). 3D image representation (b). Deformed image representation (c). Resulting contours (d).

2.3 Contour propagation

Contour propagation is performed individually for each ROI loaded from a DICOM RTSTRUCT file by following a sequence of standard image-processing operations. The mapping is always performed from the source image to the target image, such that no deformation is applied to the target image and the resulting contours are placed in the correct coordinate system.

First, the axially aligned contours defining an anatomical structure are converted into a 3D image object, by rasterizing them in to the coordinate system of the corresponding reference image. Anti-aliasing is applied in order to correctly account for partial volume effects. This image mask is then deformed non-linearly using an OpenCL accelerated GPU implementation. During the deformation, resampling to the target coordinate system with tri-linear filtering is also performed on the GPU .

This results in a deformed 3D image representation of the given structure living in the coordinate system of the target image. An additional smoothing step using a Gaussian filter kernel is applied to reduce aliasing artifacts.

Finally, result contours for each structure are generated by processing the deformed image representation slice by slice. A marching-squares algorithm with interpolation is utilized for this step. The combination of anti-aliasing during rasterization, tri-linear filtering during resampling, and interpolation in the marching-squares step assures to minimize undesired artifacts in the resulting contours. Figure 3 illustrated this process.

3 Evaluation

We have implemented our pipeline in a prototypical software assistant called *CUTE*. An initial quantitative assessment of our method was presented in [6]. Here, we present results of an in depth comparison of the performance of our method over a set of 15 structures. Eight replanning CTs of five randomly selected head and neck cancer patients have been retrospectively auto-contoured using CUTE. These contours were compared to manually created contours from

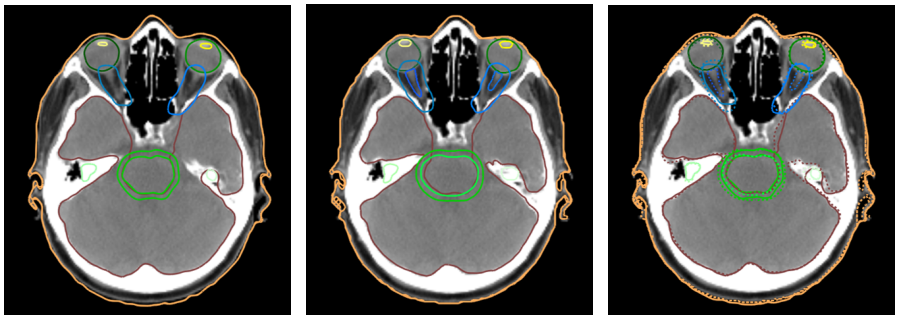

(a) (b) (c)

Fig. 4. Comparison of automatically propagated contours (a), and manually delineated contours (b). Image (c) shows both contour sets simultaneously, manual contours drawn with dashed lines.

an experienced radiotherapist. In addition, the commercially available ABAS software (Atlas-based Autosegmentation, Elekta AB, Stockholm) [1] was used to automatically create another set of contours. Then, the two automatically propagated contour sets were individually compared to the manual re-contourings. Similarly to [8] Dice similarity coefficient (DSC) and 3D Hausdorff distance (HD) were chosen as evaluation metrics. Results are shown for a subset of all contours that includes the main target volumes with nearby organs-at-risk (OARs). Target volumes have been classified to low or high depending on the patient's prescriptions dose.

4 Results

Figures 5 and 6 show box plots illustrating distribution of DSC and HD metrics of the two methods for all structures of the 8 replanning CTs. The box plot for all structures shows that both ABAS and CUTE perform well with no significant differences. Our method delivers more robust results as the quantiles are closer to the median. The best DSC-values of ABAS outperform the best ones of CUTE, yet the variation and median DSC is better in contours propagated by CUTE. Comparison of box plots created for OARs and target volumes shows that ABAS performs better for latter structures, while CUTE for the former ones. Taking a look at box plots for individual structures provides an insight into which method is superior for a given structure. We found comparable results for certain structures (e.g., larynx, PTV high) as well as significant differences for others (e.g., brainstem, mandible, both parotids).

5 Discussion and Conclusion

Our evaluation results show, that the overall quality of contouring in sense of DSC and HD is quite similar for both methods. The atlas-based method performs

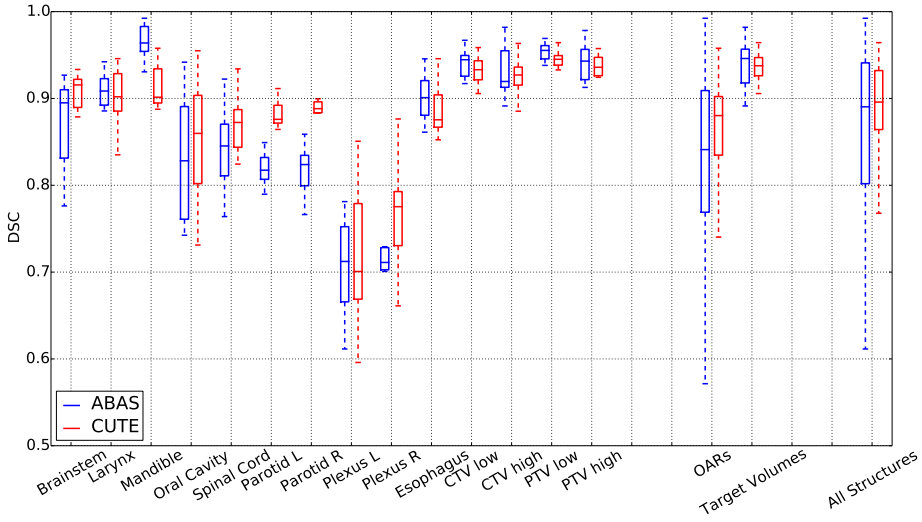

Fig. 5. Dice similarity coefficients of ABAS/CUTE contours compared to manual re-contourings.

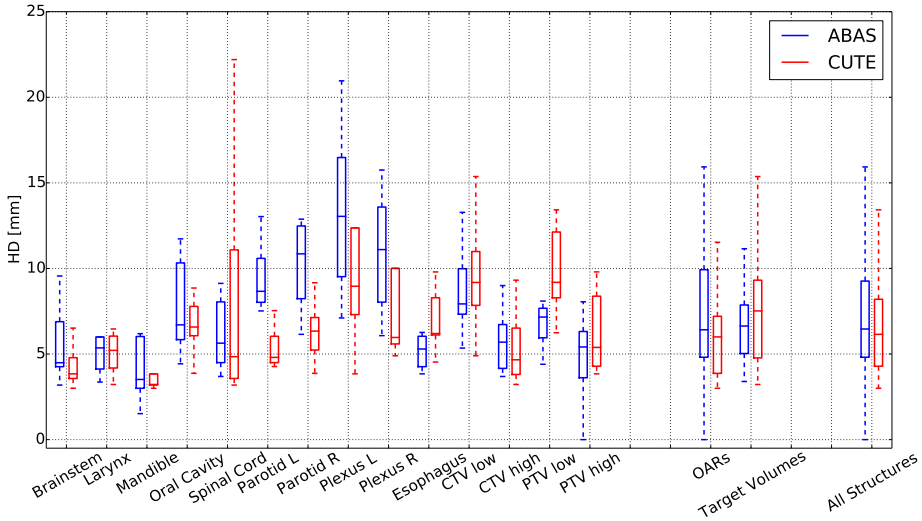

Fig. 6. Hausdorff distances of ABAS/CUTE contours compared to manual recontourings.

better than our method for target volumes resulting in higher DSC and lower HD. This is quite reasonable, considering that ABAS takes knowledge about nature of PTV into account. PTV contains large safety margins which do not correlate with the intensity values. Our registration based method cares about true image similarities and smooth transformations and not about safety margins. For OARs it is vice versa. Here only the intensity contrast and the surrounding structures rule and give an advantage to the individual registration.

Summarizing, atlas-based methods are good for bone structures and target volumes, for structures where the surroundings determine the concrete alterations, our approach performed significantly better in terms of both quality and robustness. We expect, that a combination of ABAS and CUTE could potentially optimize the overall workflow of re-planning situations in daily routine. Furthermore the fully automatic and robust approach can be performed in the background supporting automatic quantifications and dose accumulations. This will be a focus of future research.

In conclusion, contour propagation using automated mapping can be considered a reliable way to reduce the manual effort of re-contouring structures in adaptive radiation therapy.

References

1. Elekta: Atlas-based autosegmentation, http://www.elekta.com/healthcare-professionals/products/elekta-software/treatment-planning-software/contouring-software.html
2. Fischer, B., Modersitzki, J.: Curvature based image registration. Journal of Mathematical Imaging and Vision 18, 81–85 (2003)
3. Haber, E., Modersitzki, J.: Intensity gradient based registration and fusion of multimodal images. Methods of Information in Medicine 46(3), 292–299 (2007)
4. König, L., Kipshagen, T., Rühaak, J.: A non-linear image registration scheme for real-time liver ultrasound tracking using normalized gradient fields. In: Proc. MICCAI Challenge on Liver Ultrasound Tracking (CLUST 2014). Boston, USA (September 2014)
5. Modersitzki, J.: FAIR: Flexible Algorithms for Image Registration. SIAM, Philadelphia (2009)
6. Nijhuis, R., Brachmann, C., Weiler, F., Traulsen, N., Corr, D., Schenk, M., Ganswindt, U., Thieke, C., Wirtz, S., Belka, C.: A novel, efficient contour mapping method facilitates adaptive radiotherapy in head and neck patients. In: 3rd Estro Forum (2015)
7. Nocedal, J., Wright, S.J.: Numerical Optimization. Springer (1999)
8. Pekar, V., Allaire, S., Qazi, A.A., Kim, J.J., Jaffray, D.A.: Head and neck autosegmentation challenge: Segmentation of the parotid glands (2010)
9. Zhu, Y.M., Cochoff, S.M., Sukalac, R.: Automatic Patient Table Removal in CT Images. J. Digital Imaging 25(4), 480–485 (2012)